Hindawi
Shock and Vibration
Volume 2019, Article ID 8959845, 9 pages
https://doi.org/10.1155/2019/8959845

Research Article

Energy Release Analysis of a Severe Rockburst in a Headrace Tunnel Crossing a Tectonic Stress Zone

H. M. Tian[1], **W. Z. Chen**[1], **C. S. Ma**[1,2], **D. S. Yang**[1] and **X. J. Tan**[1]

[1]*State Key Laboratory of Geomechanics and Geotechnical Engineering, Institute of Rock and Soil Mechanics, Chinese Academy of Science, Beijing, China*
[2]*Patent Examination Cooperation Hubei Center of the Patent Office, CNIPA, Wuhan, China*

Correspondence should be addressed to X. J. Tan; xjtan@whrsm.ac.cn

Received 25 December 2018; Accepted 10 June 2019; Published 9 September 2019

Academic Editor: Hamid Toopchi-Nezhad

When tunneling in a hard and brittle rock mass within a tectonic stress zone, dynamic failure of rock mass-rockburst may occur. Considering the occurrence of rockburst is generally induced by a sudden release of storage elastic energy, a numerical analysis based on the geotechnical conditions of the headrace tunnels of the Neelum–Jhelum hydroelectric project was carried out to investigate the variations of the storage elastic energy of surrounding rock mass during excavation in the tectonic stress zone. As expected, the numerical results show that the storage elastic energy concentration zones is elliptical around the tunnel due to the influence of the tectonic stress field and that the long axis of the ellipse is perpendicular to the orientation of the maximum principal stress of the tectonic stress. Furthermore, the calculated storage energy concentration zone is consistent with the locations of blasting overbreak in the tunnel. Rockburst predictions were carried out using the strength-stress ratio and energy criteria to identify the applicability of the criteria in a tectonic stress zone. The comparisons between the predictions and the field observations show that the strength-stress ratio criteria based on the uniaxial tests do not consider the influence of the tectonic stress on the strength of the rock. These criteria overpredict the extent of the blasting pits in the tectonic stress zone. However, the energy criteria based on the energy conversion of unloading confining pressure tests are able to reflect the influence of the tectonic stress, and the prediction results are more close to the field observations.

1. Introduction

In recent years, in the "One Belt One Road" countries, many long and deep buried tunnels have been constructed for hydropower and transportation purposes. During the excavation of these tunnels, tectonic stress is often encountered. For example, in the headrace tunnels of the Neelum–Jhelum (N-J) hydroelectric project in Pakistan, the measured maximum principal in situ stress was greater than 100 MPa. Such in situ stress causes a number of rock mechanics problems, such as squeezing and rockburst. As the rockburst occurs instantaneously and often without any identifiable precursor, the rockburst does not only cause severe damage to the underground structures and equipment but also threaten human life. At the N-J hydroelectric project, severe rockburst in the tunnel caused the loss of several lives and extensive damage to the TBM machine.

Strain rockbursts in deep buried underground hard rock are generally characterized by a sudden release of storage elastic energy in a volume of highly stressed rock. Thus, many earlier studies focused on the variation of the storage energy in the rock mass during excavation. Cook et al. [1] first analyzed the storage energy release rate of a rock mass in a gold mine in South Africa and found that the occurrence of the rockburst is closely related to the storage energy release rate of the surrounding rock. Using the finite element method, Mitri et al. [2] investigated the seismic energy release and elastic energy storage process due to mining. They then used the ratio of the storage energy release rate to elastic energy storage rate to evaluate the rockburst potential. Wiles et al. [3] and Beck and Brady [4] analyzed the distribution and variation of the local elastic energy release density during excavation. Miao et al. [5] investigated the storage elastic energy distribution in the surrounding rock at

different overburden depths in Sanshandao Gold Mine. These studies showed that the storage elastic energy of the rock mass not only depended on the properties of the rock mass and excavation sequence but also on the magnitude of stress ratio and orientation of the in situ stress, especially in the tectonic stress zone. However, due to the difficulties in measuring the in situ stress in the field, there are few studies on the influence of tectonic stress on the distribution of storage energy of rock mass during excavation.

Many studies were carried out on predicting the rockburst to avoid the hazards of rockburst. These studies mainly used two approaches. The first is based on field tests, such as, the microseismic monitoring, which were successfully used in many deep buried tunnels [6, 7]. The second is based on the laboratory testing and theoretical analysis, including the strength-stress ratio criteria and energy criteria. The strength-stress ratio criteria [8–11] have widely been used in many tunneling projects, but the prediction results did not meet the requirements of tunneling, especially in the tectonic stress zone. The main reason is because the strength of rock used in the strength-stress ratio criteria was obtained from the laboratory axial tests, and the influence of the in situ stress on the strength of rock was not considered. The commonly used energy criteria include the linear elastic energy [12], strain energy storage coefficient [13], and rockburst energy coefficient [14]. These energy rockburst criteria are mainly based on the energy analysis of uniaxial loading or unloading tests, and the influences of in situ stress is also not considered. To reflect the influence of in situ stress, Chen et al. [15] developed a new energy criterion based on the energy conversion analysis of unloading confining pressure tests, but the applicability of this energy criterion to the tectonic stress zone has not been verified.

In this study, based on the geotechnical conditions of the headrace tunnel of the N-J hydroelectric project, a numerical analysis has been carried out to investigate the variation and distribution of the storage elastic energy in the rock mass during the tunnel excavation in the tectonic stress zone. Furthermore, the rockburst predictions have been compared with the field observations, and the applicability of different rockburst criteria to the tectonic stress zone has been investigated.

2. Introduction of N-J Headrace Tunnel

2.1. Project Description. The N-J hydroelectric project is located in the Muzaffarabad district of Azad Jammu and Kashmir, Pakistan. Two 8.53 m diameter headrace tunnels, namely, Tunnel 696 and Tunnel 697, were excavated by the TBM method for N-J hydroelectric project. The length of each tunnel is over 11 km, and 70% of the tunnel is under more than 1000 m overburden (Figure 1).

The rock mass surrounding the tunnel belongs primarily to Murree Formation, which comprises alternating beds of sandstone, siltstone, mudstone, and shale. The sandstone is well cemented, fine to medium grained, and the main compositions of the sandstone are shown in Table 1. According to the results of the laboratory tests, the uniaxial compression strength of the sandstone varies between 120 and 170 MPa with a mean strength of 145 MPa.

During the excavation of the Tunnel 696, hundreds of weak and medium rockbursts occurred in the sandstone since the buried depth reached and exceeded 800 m, and a severe rockburst occurred at chainage 09 + 700~800. This severe rockburst caused loss of several lives and extensive damage to the TBM machine. The tunnel profile after the severe rockburst is shown in Figure 2. It can be seen that the overbreak due to the burst primarily involved the crown between 10 and 12 o'clock and much lesser extent at the invert between 4~6 o'clock of the tunnel. The average depth of the overbreak at the crown is 3.0~4.0 m, and the maximum depth is more than 6.0 m.

2.2. Tectonic Stress. The N-J project is located in the Himalayas Mountain, and local faults have been developed along the TBM tunnel. The geological investigation has shown that severe rockburst occurred in the vicinity of a local reverse fault. Stress measurement was carried out to investigate the in situ stress of this area. Three overcoring HI (hollow inclusion) tests were conducted in the borehole at chainages 9 + 860, 10 + 938, and 13 + 834 in Tunnel 696 (Figure 1). The tests at chainage 9 + 860 failed due to the core discing (Figure 3), which indicates high in situ stress of this area. The HI tests at chainages 10 + 938 and 13 + 834 are successful, and the rock core of HI cells is shown in Figure 4. In each borehole, three HI tests were carried out in different depths of the borehole, and all results are shown in Table 2. It can be seen that although the overburden depth at chainage 10 + 938 is only 200 m more than that at chainage 13 + 834, the maximum principal stress increases from 50–55 MPa to 102–108 MPa. This significant increase in the in situ stress is due to the local reverse fault. The orientation of the principal stresses at chainage 10 + 938 is drawn in the lower hemisphere stereonet in Figure 5. It can be seen that the orientation of the maximum principal stress is almost perpendicular to the tunnel axis, and its dip is among 20° to 30° from the horizontal plane, indicating that the horizontal tectonic stress field dominates in this area.

3. Variations of Storage Elastic Energy of Rock Mass in the Tectonic Stress Zone

The occurrence of rockburst is induced by a sudden release of storage elastic energy in the surrounding rock. In order to investigate the influence of tectonic stress on the distribution and magnitude of storage elastic energy, a numerical analysis has been carried out based on the geotechnical conditions in the severe rockburst zone in Tunnel 696.

3.1. Numerical Model. Using a finite element method, a numerical model has been developed as shown in Figure 6. And the model is established based on the geotechnical conditions at chainage 09 + 700~800 in Tunnel 696, where a severe rockburst occurred. The length, height, and width of the model are 100 m, 120 m, and 200 m, respectively. The elastic-perfect plastic model is used to describe the behavior of the rock mass, and the mechanical parameters of the rock mass determined by triaxial compression tests of sandstone are shown in Table 3. Since the tectonic stress in this area is high, the mean measured in situ

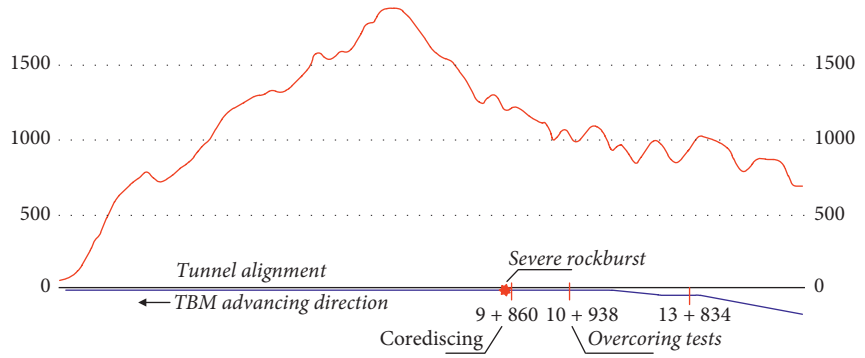

Figure 1: Tunnel profile with the range of rock cover.

Table 1: Composition of sandstone in the N-J headrace tunnel.

Quartz (%)	Potassium feldspar (%)	Albite (%)	Calcite (%)	Dolomite (%)	Hematite (%)	Clay mineral (%)
38.9	0.4	3.7	33.8	6.6	1.2	15.4

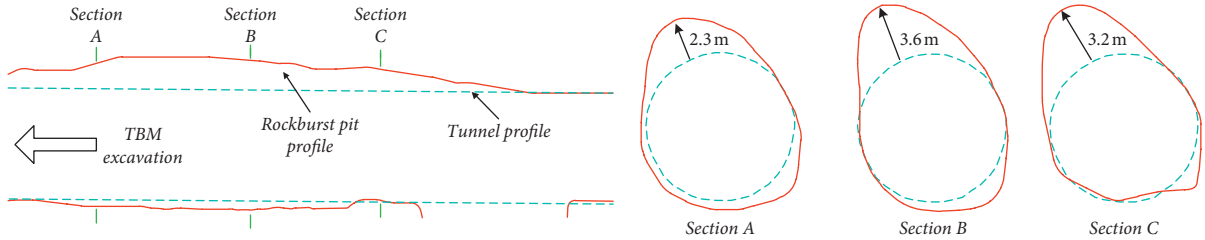

Figure 2: Measured blasting pits profile in Tunnel 696. (a) Longitudinal section and (b) cross section of the tunnel.

Figure 3: Core discing in the borehole at chainage 9 + 860.

stress at chainage 10 + 938 in Tunnel 696 has been applied to the numerical analysis, and the stress components of the in situ stress in the local coordinate system of the tunnel are shown in Table 4. In order to apply the shear stress components of the in situ stress, a combined stress and deformation boundaries were applied on the model.

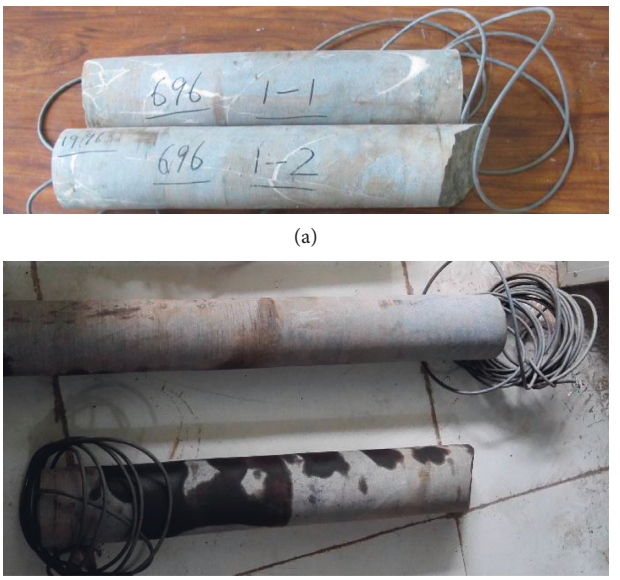

Figure 4: Rock core of HI cells: (a) chainage 10 + 938 and (b) chainage 13 + 834.

Table 2: Stress test results at chainage 10 + 938 and 13 + 834.

Chainage	Buried depth	Tests no	Depth in borehole (m)	σ_1/Tr/Pl (MPa/°/°)	σ_2/Tr/Pl (MPa/°/°)	σ_3/Tr/Pl (MPa/°/°)
13 + 834	800	1	23.0	−50.7/282/−14	−24.3/206/43	−19.5/358/44
		2	24.3	−54.9/287/−30	−27.7/204/13	−21.2/315/57
		3	25.9	−50.7/281/−39	−21.3/210/22	−15.9/322/43
10 + 938	1010	1	19.1	−102.9/292/33	−40.6/193/14	−25.1/84/54
		2	20.0	−107.3/338/21	−40.9/119/64	−32.7/243/13
		3	21.0	−102.9/312/32	−48.4/195/47	−24.4/70/37

Plunge (dip) from horizontal positive down and trend (azimuth) positive clockwise from north.

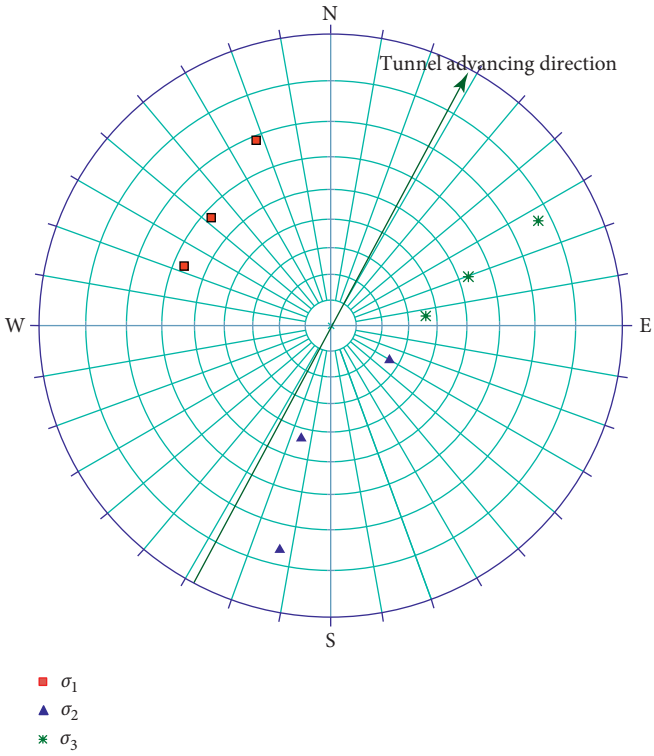

Figure 5: Orientation of principle stresses at chainage 10 + 938 in the lower hemisphere stereonet (σ_1, σ_2, and σ_3 are the maximum principle stress, intermediate principal stress, and the minimum principle stress of the in situ stress, respectively).

Using the established finite element model to carry out a numerical analysis, the procedure is as follows:

Step 1. Apply the in situ stress.

Step 2. Excavate the headrace tunnel step by step, and the excavation length of each step is 5 m.

3.2. Influence of Tectonic Stress on Storage Elastic Energy. After the excavation of the tunnel, the distribution of the storage elastic energy density of the rock mass at typical cross section is shown in Figure 7. It can be seen that there are storage elastic energy concentrations at 10~12 o'clock of the tunnel vault and at 4~6 o'clock of the tunnel invert. The storage elastic energy concentration zone is elliptical around the tunnel, which is consistent with the distribution of the blasting pit in the field, meaning that the occurrence of rockburst is closely related to the concentration of storage elastic energy in the tectonic stress zone.

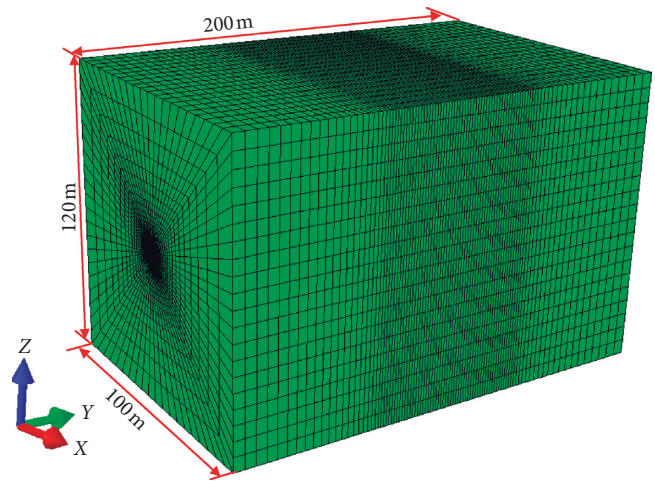

Figure 6: Numerical model of the severe rockburst zone in Tunnel 696.

The orientation of the principal stresses of the tectonic stress is shown in Figure 8 to investigate the influence of tectonic stress on the distribution of storage elastic energy. The line between storage elastic energy concentration zones is elliptical around the tunnel due to the influence of the tectonic stress, and the long axis of the ellipse is perpendicular to the orientation of the maximum principal stress and parallel to the orientation of the minimum principal stress. Hence, it can be concluded that during the tunnel excavation, the concentration of the storage elastic energy is mainly induced by the loading at the maximum principal stress orientation and unloading at the minimum principal stress orientation.

The variation of the magnitude of storage elastic energy at the tunnel vault is shown in Figure 9 to investigate the tectonic stress on the magnitude of storage elastic energy. It can be seen that the storage elastic energy of the rock mass is composed of two parts. One is the initial storage energy before the excavation of the tunnel induced by the tectonic stress. The initial storage energy is a constant in this zone. Due to tectonic stress, the initial storage elastic energy density of the rock mass in this zone is up to 210 kJ/m^3. Another part is the storage elastic energy induced by the stress redistribution due to the tunnel excavation, and its value varies from the location of the rock mass and the excavation process. For the rock mass near the tunnel profile, the elastic energy of the rock mass first increases with

Table 3: Mechanical parameters of sandstone and shotcrete.

Materials	Young's modulus (GPa)	Poisson's ration	Cohesive strength (MPa)	Friction angle (°)
Sandstone	20	0.25	4.3	42
Shotcrete	25	0.2	—	—

Table 4: Mean values of stress components in the local coordinate system (measurement results at chainage 10 + 938).

σ_{xx}	σ_{yy}	σ_{zz}	τ_{yz}	τ_{xz}	τ_{xy}
−83.8	−44.7	−47.8	−2.0	−26.0	12.7

Stress positive-negative regularity follows linear elastic mechanics. Positive normal stress is tensile stress, and negative is compressive stress. The direction of local coordinate is shown in Figure 5.

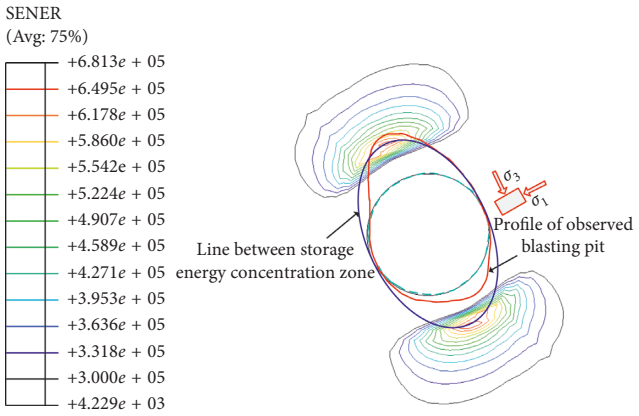

Figure 7: Distribution of the storage elastic energy density of the rock mass after excavation (unit: J/m3).

the tunnel excavation and then decreases significantly when the TBM passes through. The decrease of the elastic energy is mainly due to the plastic dissipation of the rock mass. For the rock mass far away from the tunnel profile, there is no plastic strain, and the elastic energy is always increasing with the tunnel excavation. When the excavation face advances 10–15 m, the storage elastic energy of rock mass tends to be a constant and with a maximum value of 680 kJ/m^3. It can be seen that the initial storage elastic energy of the rock mass induced by the tectonic stress is up to 30% of the total storage elastic energy after excavation. This explains why the rockburst is likely to occur in the tectonic stress zone.

4. Rockburst Predictions in the Tectonic Stress Zone in Tunnel 696

Predictions of severe rockburst potential in Tunnel 696 were carried out to investigate the applicability of the strength-stress ratio and energy rockburst criteria in a tectonic stress zone, and the predictions results have been compared with the field observations of the blasting pits.

4.1. Predictions of Severe Rockburst Using Strength-Stress Ratio Criteria. The commonly used strength-stress ratio criteria are shown in Table 5. In the tectonic stress zone of Tunnel 696, the mean value of maximum principal in situ stress σ_1 is

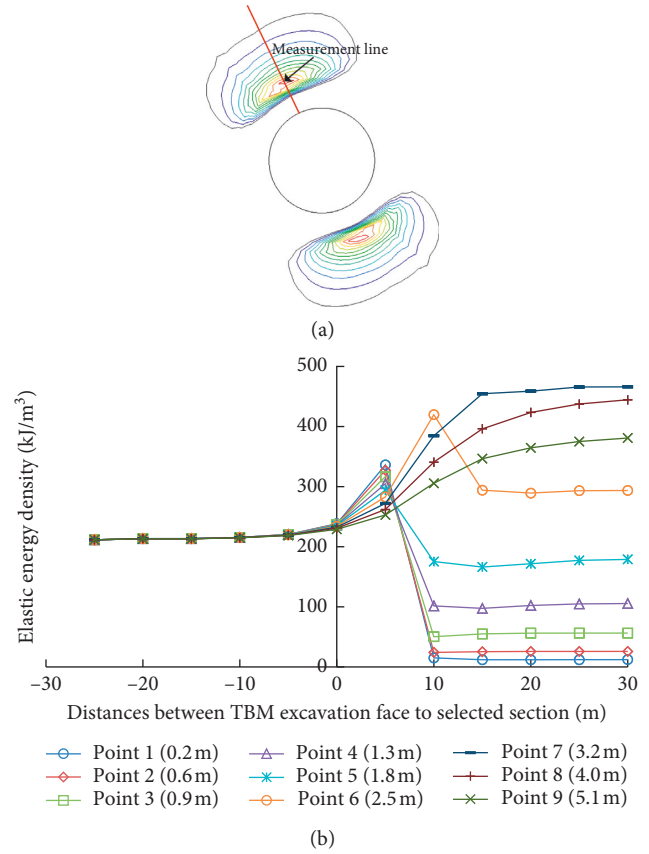

Figure 8: Variation of the storage elastic energy during tunnel excavation. (a) Location of the measurement line. (b) Variation of the storage elastic energy of rock mass on the measurement line.

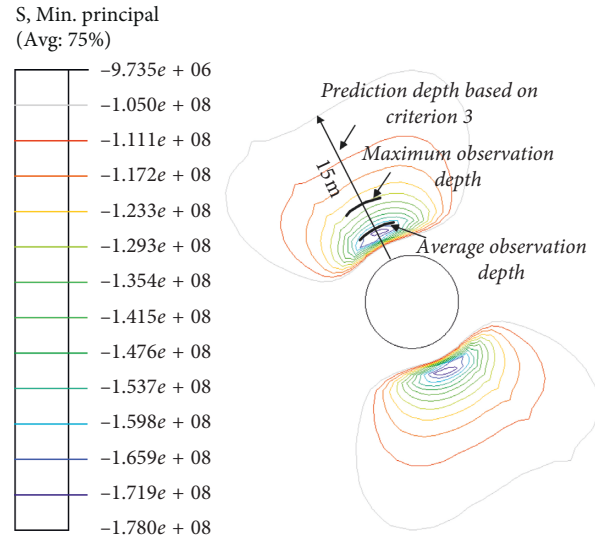

Figure 9: Prediction results of distribution and extent of sever rockburst using strength-stress ratio criteria.

Table 5: Commonly used strength-stress ratio criteria.

Criteria	Proposer	Formula	Rockburst grade			
			No	Light	Moderate	Severe
1	[16]	σ_{ci}/σ_h	>7.0	4.0~7.0	2.0~4.0	<2.0
2	[8]	σ_{ci}/σ_1	>10.0	10.0~5.0	5.0~2.5	<2.5
3	[11]	$\sigma_{\theta max}/\sigma_{ci}$	0.34	0.42	0.56	0.70
4	[9]		≤0.20	0.20~0.30	0.30~0.55	≥0.55

σ_{ci} is the compressive strength of rock obtained from laboratory uniaxial tests; $\sigma_{\theta max}$ is the maximum principle stress of rock mass after excavation; σ_1 is the maximum principal stress of in situ stress; σ_h is the horizontal stress component of in situ stress perpendicular to the tunnel alignment.

104.4 MPa, and the mean horizontal stress component of the in situ stress perpendicular to the tunnel alignment σ_h is 83.8 MPa. Based on Criteria 1 and 2, severe rockburst will occur in the tectonic stress zone in Tunnel 696 ($\sigma_{ci}/\sigma_h = 1.7$ and $\sigma_{ci}/\sigma_1 = 1.4$), which are consistent with the field observations. However, the distribution and extent of blasting pits cannot be predicted by these two criteria.

Based on the numerical results of stress distribution of surrounding rock after excavation, the predictions of the distribution and extent of severe rockburst used the Criteria 3 and 4 are shown in Figure 8. It can be seen that the predicted severe rockburst is located between 10 and 12 o'clock of the tunnel vault and 4 and 6 o'clock of tunnel invert, and they are symmetrical. As the blasting depth at the tunnel invert cannot be measured accurately, only the extent of the rockburst at the tunnel vault has been compared with the field measurements. It can be seen that the predicted rockburst location is consistent with the observation in Tunnel 696. However, the maximum extent of the predicted rockburst is up to 15.0 m (Criteria 3) and 20.0 m (Criteria 4), which is much larger than that in the field observation (6.0 m). This shows that the extent of the blasting pit is overpredicted in the tectonic stress zone. The overprediction is mainly due to the strength of the rock used in the strength-stress ratio criteria, which is obtained from the laboratory axial tests, and the influence of the in situ stress on the strength of the rock is not considered. As such, the strength of the rock mass far away from the tunnel profile is underestimated, and the extent of the blasting pit is overstated especially in the tectonic stress zone.

4.2. Predictions of Severe Rockburst Using Energy Criteria. The commonly used energy criteria include the linear elastic energy, strain energy storage coefficient, and rockburst energy coefficient. They are based on the energy analysis of uniaxial loading or unloading tests and do not consider the influences of tectonic stress. In this study, the energy criterion based on the unloading confining pressure tests has been used [15]:

$$\frac{U^e}{U^{e-max}} = \begin{cases} 0.3, & \text{weak rockburst,} \\ 0.4, & \text{medium rockburst,} \\ 0.5, & \text{strong rockburst,} \\ \geq 0.7, & \text{severe rockburst,} \end{cases} \quad (1)$$

where U^{e-max} is the maximum storage elastic energy of rock before its failure obtained from unloading confining pressure tests and U^e is the storage elastic energy of rock mass due to in situ stress and the excavation of the tunnel.

4.2.1. Identification of Maximum Storage Elastic Energy. To identify the maximum storage elastic energy of sandstone in Tunnel 696, a series of unloading confining pressure tests have been carried out. The cylindrical samples (100 mm long and 50 mm in diameter) for the unloading tests were machined from a large lump of rock mass, and the specimen is shown in Figure 10. The unloading confining pressure tests were conducted on the MTS 815.03 compression tests machine, at the State Key Laboratory of Geomechanics and Geotechnical Engineering, Institute of Rock and Soil Mechanics. The procedure of the unloading tests is as follows:

Step 1. Apply the initial hydrostatic pressure. The confining pressure is applied first at the rate of 1 MPa/s, and the axial stress is applied simultaneously to keep the sample subjected to hydrostatic pressure.

Step 2. Apply the initial axial stress. To obtain the maximum storage elastic strain energy of the sandstone, an initial axial stress is applied first to ensure the failure behavior of the specimen occur during the unloading process. In this study, the initial axial stress is 70% of the triaxial strength of the specimen.

Step 3. Unload the confining pressure. The confining pressure is unloaded by the stress-controlled way at the design unloading rate. Meanwhile, the axial stress is increased at the same rate, to coordinate the stress variation of the surrounding rock mass during the excavation of the tunnel. Considering the excavation of the rock mass can be treated as a quasi-static process, the unloading rate of the confining pressure is at a low level with a mean 0.125 MPa/s.

The typical stress-strain curve of the sandstone during the unloading tests is shown in Figure 11, and the storage process of elastic energy is divided into three parts as follows:

$$U^e = U_h^e + U_l^e + U_u^e, \quad (2)$$

where U_h^e is the storage elastic energy during the application of the hydrostatic pressure, U_d^e is the storage elastic energy during the application of the initial axial stress, and U_u^e is the storage elastic energy during unloading confining pressure.

Generally, the specimen is in the elastic stage during the application of the hydrostatic pressure, and the storage elastic strain energy U_h^e can be directly calculated as follows:

$$U_h^e = \frac{3(1-2\mu)(\sigma_3^0)^2}{2E}, \quad (3)$$

where μ is Poisson's ratio, E is the elastic modulus of the rock specimen and σ_3^0 is the initial confining pressure.

During the application of the initial axial stress, the axial stress is lower than 70% of triaxial strength of the specimen, and the specimen is in the elastic range. Hence, the storage elastic energy U_d^e can be calculated as follows:

Figure 10: Rock specimens for unloading confining pressure tests.

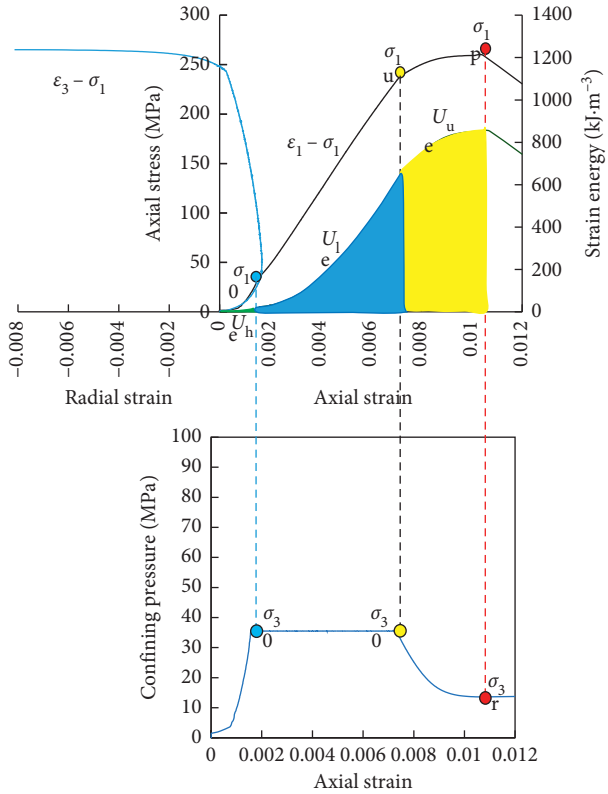

Figure 11: Typical stress-strain curve of sandstone during unloading confining pressure tests.

$$U_l^e = \frac{1}{2E}\left[(\sigma_1^u)^2 - (\sigma_3^0)^2 - 4\mu\left(\sigma_1^u\sigma_3^0 + (\sigma_3^0)^2\right)\right]. \quad (4)$$

During the unloading process, the storage elastic energy U_u^e is

$$U_u^e = \frac{1}{2E_u}\left[(\sigma_1^p)^2 + 2(\sigma_3^r)^2 - 2\mu_u\left(2\sigma_1^p\sigma_3^r + (\sigma_3^r)^2\right)\right] - \frac{1}{2E}\left[(\sigma_1^\mu)^2 + 2(\sigma_3^0)^2 - 2\mu\left(2(\sigma_1^\mu)^2\sigma_3^0 + (\sigma_3^0)^2\right)\right], \quad (5)$$

where E_u and μ_u are the unloading elastic modulus and Poisson's ratio of the specimens. According to Huang and Li [17], E_u is 5–8% larger than the elastic modulus E, and μ_u is about 3–6% smaller than Poisson's ratio μ. In this study, $E_u = 1.07\,E$, and $\mu_u = 0.96\,\mu$.

According to the above analysis, the storage elastic energy of the specimen can be determined from the elastic parameters E and μ. Assuming that the specimen is in the elastic range during the application of the initial axial stress, the parameters E and μ for each specimen can be estimated from its stress-strain curve, and their values are shown in Table 6. Substituting the elastic parameters into equations (3)~(5), the maximum storage elastic energy of the specimen has been calculated and shown in Table 6.

To investigate the influences of the initial confining pressure on the maximum storage elastic energy of the rock, the variations of the maximum storage elastic energy with the initial confining pressure are shown in Figure 12. It can be seen that the initial confining pressure has an important influence on U^{e-max}, and similar results were also observed by Urbancic and Trifu [18]. For a quantitative analysis on the influence of the initial confining pressure, the maximum storage elastic energy of the specimens under the uniaxial test (the confining pressure is 0 MPa) is also shown in Figure 12. This figure also shows the fitting of the data to an exponential curve, and the fitted exponential equation is

$$U^{e-max} = 275.7\exp\left(0.0285 * \sigma_3^0\right). \quad (6)$$

As the correlation coefficient is greater than 0.95, this means that the exponential model is a good fit between U^{e-max} and the initial confining pressure.

4.2.2. Predictions of Severe Rockburst Using Storage Energy Criteria. According to the analysis on the variations of the storage elastic energy during the excavation of the tunnel, the concentration of the storage elastic energy around the tunnel is induced by the loading at the maximum principal stress orientation and unloading at the minimum principal stress orientation. Considering the loading path of the unloading confining pressure tests, the minimum principal stress of the in situ stress can be treated as the initial confining pressure, and the maximum storage elastic energy of a rock mass can be calculated using equation (6). The mean minimum principal stress of the tectonic stress zone is 27.3 MPa, and the maximum storage elastic energy of surrounding rock is calculated as 601 kJ/m^3.

According to the energy criterion developed by Chen et al. [15];when the elastic energy of a rock mass is greater than 300.5 kJ/m^3 (i.e., 0.5×601 kJ/m^3), severe rockburst will occur. Furthermore, according to the numerical results, the distribution of the severe rockburst is shown in Figure 13. It can be seen that the predicted severe rockburst zone is also located between 10 and 12 o'clock and 4 and 6 o'clock of the tunnel. However, the extent of the severe rockburst is much smaller than that of the predictions using the strength-stress ratio criteria. The extent of the maximum prediction blasting pit at the tunnel vault is about 6.8 m, which is close to the measured blasting pit at the tunnel vault (6.0 m). This shows that the prediction by the energy criterion based on the energy conversion of the unloading confining pressure tests is more accurate than that by the strength-stress ratio criteria in the tectonic stress zone.

Table 6: Results of unloading confining pressure tests of sandstone.

Initial confining pressure (MPa)	Tests no.	Young's modulus (GPa)	Poisson's ration	Peak deviatoric stress (MPa)	Maximum storage elastic energy (kJm^{-3})
35	1	40.2	0.26	250	820.0
	2	35.9	0.22	245	866.5
	3	38.3	0.24	246	833.4
45	4	34.2	0.23	269	1114.3
	5	40.3	0.24	282	1053.1
	6	51.7	0.27	283	898.0
55	7	32.1	0.22	267	1363.9
	8	32.8	0.24	286	1445.8
	9	32.7	0.23	285	1434.0
65	10	52.4	0.28	336	1667.5
	11	29.1	0.21	329	1909.8
	12	30.8	0.24	301	1788.8
75	13	28.0	0.23	338	2233.2
	14	35.0	0.25	357	2097.9
	15	38.3	0.25	353	1801.8

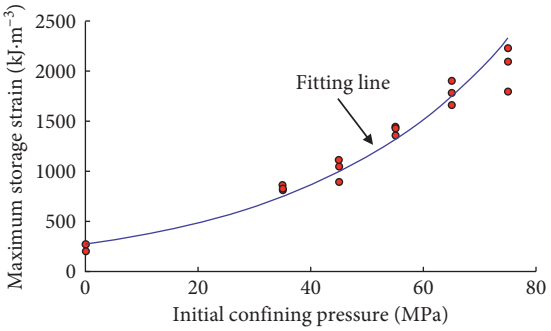

Figure 12: Variations of the maximum storage elastic energy of sandstone with initial confining pressure.

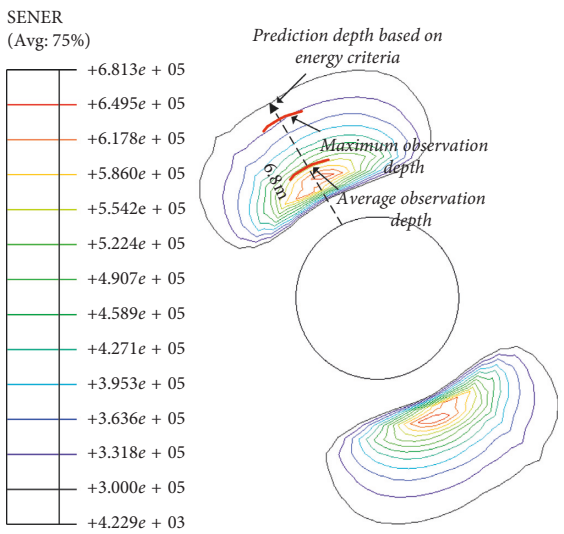

Figure 13: Prediction results of distribution and extent of sever rockburst using energy criteria.

5. Conclusions

In this study, by applying a numerical model to the geotechnical conditions in the headrace tunnels of N-J hydroelectric project, a numerical analysis has been carried out to investigate the variations of the storage elastic energy of a rock mass in the tunnel at the tectonic stress zone. The numerical results show that the line between storage energy concentration zones is elliptical around the tunnel due to the influence of the tectonic stress. The long axis of the ellipse is perpendicular to the orientation of the maximum principal stress of the tectonic stress. Furthermore, the calculated storage energy concentration zone is consistent with the locations of the blasting pits at the tunnel vault in the field. Besides, in a tectonic stress zone, the initial storage elastic energy induced by the tectonic stress is up to 30% of the total storage elastic energy after excavation. This means that the tectonic stress clearly increases the risk of rockburst.

To identify the applicability of rockburst criteria to a tectonic stress zone, different types of criteria have been used to predict rockburst in Tunnel 696. The comparisons between the predictions and the field observations show that the strength-stress ratio criteria overpredict the extent of the blasting pits in the tectonic stress zone. The overprediction is mainly due to the strength of the rock used in the strength-stress ratio criteria is obtained from the laboratory axial tests, and the influence of the in situ stress on the strength of the rock is not considered. The energy criteria based on the energy conversion of unloading confining pressure tests are able to reflect the influence of the tectonic stress (i.e., the initial confining pressure), and the prediction results are close to the field observations, indicating that the energy criteria are more applicable in a tectonic stress zone.

Data Availability

All data included in this study are available from the corresponding author upon request.

Conflicts of Interest

The authors declare that they have no conflicts of interest.

Acknowledgments

The authors gratefully acknowledge the support of the Youth Innovation Promotion Association CAS.

References

[1] N. G. W. Cook, E. Hoek, J. P. G. Pretorius et al., "Rock mechanics applied to the study of rockbursts," *Journal of the South African Institute of Mining and Metallurgy*, vol. 66, pp. 436–528, 1966.

[2] H. S. Mitri, B. Tang, and R. Simon, "FE modelling of mining-induced energy release and storage rates," *The Journal of the South African Institute of Mining and Metallurgy*, vol. 99, no. 2, pp. 103–110, 1999.

[3] T. D. Wiles, S. D. Marisett, and C. D. Martin, "Correlation between local energy release density observed bursting conditions at Creighton mine," Mine Modeling Report, Creighton Mine, Sudbury, Canada, 1998.

[4] D. A. Beck and B. H. G. Brady, "Evaluation and application of controlling parameters for seismic events in hard-rock mines," *International Journal of Rock Mechanics and Mining Sciences*, vol. 39, no. 5, pp. 633–642, 2002.

[5] S.-J. Miao, M.-F. Cai, Q.-F. Guo, and Z.-J. Huang, "Rock burst prediction based on in-situ stress and energy accumulation theory," *International Journal of Rock Mechanics and Mining Sciences*, vol. 83, pp. 86–94, 2016.

[6] C. A. Tang and P. K. Kaiser, "Numerical simulation of cumulative damage and seismic energy release during brittle rock failure-part I: fundamentals," *International Journal of Rock Mechanics and Mining Sciences*, vol. 35, no. 2, pp. 113–121, 1998.

[7] T. H. Ma, C. A. Tang, L. X. Tang, W. D. Zhang, and L. Wang, "Rockburst characteristics and microseismic monitoring of deep-buried tunnels for Jinping II hydropower station," *Tunnelling and Underground Space Technology*, vol. 49, pp. 345–368, 2015.

[8] N. Barton, R. Lien, and J. Lunde, "Engineering classification of rock masses for the design of tunnel support," *Rock Mechanics*, vol. 6, no. 4, pp. 189–236, 1974.

[9] B. F. Russenes, "Analysis of rock spalling for tunnels in steep valley sides (in Norwegian)," M.Sc. thesis, Norwegian Institute of Technology, Dept. of Geology, Trondheim, Norway, 1974.

[10] I. A. Turchaninov, "Interrelation between the stressed state of rocks and their properties," *Soviet Mining Science*, vol. 14, no. 2, pp. 140–144, 1978.

[11] E. Hoek and E. T. Brown, *Underground Excavations in Rock*, Institution of Mining and Metallurgy, London, UK, 1980.

[12] C. Qiao and Z. Tian, "Possibility of rockburst occurrence in Dongguashan copper deposit," *Chinese Journal of Rock Mechanics and Engineering*, vol. 17, pp. 917–921, 1998, in Chinese.

[13] A. Kidybiski, "Bursting liability indices of coal," *International Journal of Rock Mechanics and Mining Sciences & Geomechanics Abstracts*, vol. 18, no. 4, pp. 295–304, 1981.

[14] R. E. Goodman, *Introduction to Rock Mechanics*, Wiley, New York, NY, USA, 1980.

[15] W. Z. Chen, S. P. Lu, X. H. Guo, and C. J. Qiao, "Research on unloading confining pressure tests and rockburst criterion based on energy theory," *Chinese Journal of Rock Mechanics and Engineering*, vol. 28, no. 8, pp. 1530–1540, 2009, in Chinese.

[16] Ministry of Construction of the PRC, *Code for Geological Survey of Water Resources and Hydropower Projects*, China Planning Press, Beijing, China, 2009.

[17] D. Huang and Y. Li, "Conversion of strain energy in triaxial unloading tests on marble," *International Journal of Rock Mechanics and Mining Sciences*, vol. 66, pp. 160–168, 2014.

[18] T. I. Urbancic and C.-I. Trifu, "Recent advances in seismic monitoring technology at Canadian mines," *Journal of Applied Geophysics*, vol. 45, no. 4, pp. 225–237, 2000.